

# CSMAE : CATARACT SURGICAL MASKED AUTOENCODER (MAE) BASED PRE-TRAINING

*Nisarg A. Shah*<sup>1</sup>

*Wele Gedara Chaminda Bandara*<sup>1</sup>

*Shameema Skider*<sup>2,3</sup>

*S. Swaroop Vedula*<sup>3</sup>

*Vishal M. Patel*<sup>1</sup>

<sup>1</sup> Johns Hopkins University, Baltimore, USA

<sup>2</sup> Wilmer Eye Institute, Johns Hopkins University, Baltimore, USA

<sup>3</sup> Malone Center for Engineering in Healthcare, Johns Hopkins University, Baltimore, USA

## ABSTRACT

Automated analysis of surgical videos is crucial for improving surgical training, workflow optimization, and postoperative assessment. We introduce a CSMAE, Masked Autoencoder (MAE)-based pretraining approach, specifically developed for Cataract Surgery video analysis, where instead of randomly selecting tokens for Masking, they are selected based on spatiotemporal importance of the token. We created a large dataset of cataract surgery videos to improve the model’s learning efficiency and expand its robustness in low-data regime. Our pre-trained model can be easily adapted for specific downstream tasks via fine-tuning, serving as a robust backbone for further analysis. Through rigorous testing on downstream step—recognition task on two Cataract surgery video datasets, D99 and Cataract-101—our approach surpasses current state-of-the-art self-supervised pre-training and adapter-based transfer learning methods by a significant margin. This advancement not only demonstrates the potential of our MAE-based pretraining in the field of surgical video analysis but also sets a new benchmark for future research.

**Index Terms**— Video Pre-training, Cataract Surgery, Transformer

## 1. INTRODUCTION

Recent advances in medical imaging show the effectiveness of Transformer pre-training on large datasets for classification, detection, and segmentation. Due to the variety of imaging types and high data costs, models tailored to specific data are often necessary [1, 2]. Our research focuses on cataract surgical videos, essential for eye disease diagnosis, training, and minimally invasive surgeries.

Medical imaging often combines images and text, as seen in X-ray diagnosis [3] and radiology report generation [4] with vision-language models. However, cataract videos lack text, requiring image/video-only models. Tasks like step recognition need a lot of expert-labeled data, which is hard to obtain[5]. We propose CSMAE, a self-supervised learning approach using masked autoencoders (MAE) to pre-train on unlabeled cataract videos, enabling feature learning for step recognition.

Self-supervised learning includes two main strategies: 1) Contrastive Learning [6, 7] and 2) Masked Autoencoders (MAEs) [8, 9]. Contrastive learning compares augmented image versions, clustering similar images and distancing different ones in latent space. MAEs, in contrast, divide an image or video into patches, mask some randomly, and reconstruct them using features from unmasked patches. MAEs use a Vision Transformer (ViT) [10, 11] encoder for visible patches and a lightweight decoder for prediction. MAEs are particularly effective, as they learn from incomplete data and outperform contrastive learning on multiple tasks.

We developed a video transformer model to encode patches, inspired by the ViT-B architecture in VideoMAE [9]. In training, we tested various masking techniques—random, tube, and frame—with random masking showing improved results. However, since not all patches hold equal information, random sampling can overlook key spatiotemporal cues. To address this, our approach selects patches based on their spatiotemporal significance rather than standard random sampling as proposed in [12] for general vision videos. An auxiliary network defines a categorical distribution across input tokens, from which visible tokens are sampled, ensuring a more focused, informative selection.

In this work, we show the effectiveness of the MAE-based approach for Vision Transformer pretraining in cataract videos with the following contributions: (1) An end-to-end token sampling strategy that selects high-informative spatiotemporal tokens, discarding redundant ones for efficient MAE pre-training on long cataract surgery videos; (2) Improved GPU memory efficiency and enhanced feature learning as the CSMAE model focuses on spatiotemporal-rich regions; and (3) Extensive evaluation of the CSMAE pre-trained model on Step Recognition, demonstrating its effectiveness in both semi-supervised and supervised settings.

## 2. THE CSMAE MODEL

Fig. 1 shows the CSMAE framework similar to [12, 9], composed of four main components: a Tokenizer, Encoder, Decoder, and a Token Selection Network.

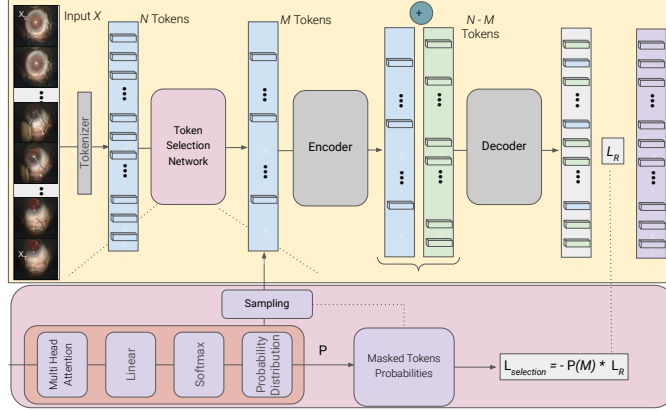


**Fig. 1.** The CSMAE model, developed on an encoder-decoder framework, consists of four principal components: a Tokenizer, Token Selection Network, an Encoder, and a Lightweight Decoder. The Tokenizer converts raw video data into a token-based feature representation. Utilizing transformer architecture, the Token Selection Network predicts the probability distribution for each token, choosing those with significant spatiotemporal information to feed into the Encoder. This Encoder, which employs the ViT network, captures the feature representation of these selected tokens. These representations are then combined with learnable feature representations of masked tokens, aiming to reconstruct the masked feature representation accurately.

**Tokenizer:** For a video input  $X$  of dimensions  $T \times C \times H \times W$  (temporal frames, RGB channels, and spatial dimensions), the Tokenizer [9] uses a 3D convolution layer to convert  $X$  into  $N$  tokens, each with dimension  $k$ , and applies positional encoding [8, 9].

**Token Selection Network:** Following [12], the Tokenizer output  $T$  is processed through a Multi-Head Attention (MHA) layer, a Linear layer, and Softmax to generate probability scores  $P$  for each token:

$$P = \text{Softmax}(\text{Linear}(\text{MHA}(T))).$$

An  $N$ -dimensional categorical distribution is applied to  $P$ , selecting a subset  $M_i$  of visible tokens based on a masking ratio  $\alpha \in (0, 1)$ .

**Encoder:** The encoder processes selected visible tokens  $T_v$  via a ViT encoder to produce latent representations  $F_v$ .

**Decoder:** The decoder combines  $F_v$  with a fixed representation for masked tokens using positional encoding. A transformer then reconstructs the masked video frames  $X_{n-m}$ .

## 2.1. Training CSMAE

**Masked Reconstruction Loss  $L_R$ :** We use Mean Squared Error (MSE) loss between predicted masked tokens  $X_b$  and ground-truth normalized RGB values  $X_e$ :

$$L_R(\phi) = \frac{1}{N - M} \sum_{i \in M'_i} \|X_{b_i} - X_{e_i}\|^2,$$

where  $X_b$  are the predicted tokens, and  $X_e$  is the ground-truth.

**Token Selection Loss  $L_{select}$ :** We train the token selection mechanism, parameterized by  $\theta$ , using a sampling loss  $L_{select}$  based on the Gradient-Following algorithm [23, 12]

from reinforcement learning. This approach treats token selection as actions within an MAE environment, with the masked reconstruction loss  $L_R$  as the return. The goal is to maximize the expected reconstruction error  $E[L_R]$ , akin to maximizing expected rewards.

Following compressed sensing principles, tokens are sampled more heavily in high-activity regions, allowing for masking ratios up to 95% and leading to efficient sampling and reduced computational load. This strategy enables faster pre-training by concentrating tokens in high-information areas.

The objective function for optimizing token selection is:

$$L_{select}(\theta) = -E_\theta[L_R(\phi)] = - \sum_{i \in I_m} P_{i\theta} \cdot L_{iR}(\phi),$$

where  $P_{i\theta}$  is the token selection probability for index  $i$ , and  $L_{iR}$  is the reconstruction error for each masked token [12]. To isolate MAE parameters ( $\phi$ ) from  $L_{select}(\theta)$ , gradient updates are detached, and logarithmic scaling is applied to probabilities to address precision issues.

## 3. EXPERIMENTS AND RESULTS

**Datasets.** For pre-training, we extend the D99 dataset to create D450, adding 350 cataract surgery videos for a total of 450 videos, each averaging 34 minutes at 59  $fps$ . We evaluate CSMAE on two untrimmed cataract datasets: Cataract-101 [24] and D99 [25]. For Step Recognition fine-tuning, we experiment with both low-data and full-data settings. The D99 dataset has 99 videos with 12 annotated steps, a  $640 \times 480$  resolution, and 59  $fps$ . Following [5], we split D99 into 60, 20, and 19 videos for training, validation, and testing. Cataract-101 includes 101 videos at 25  $fps$  with 10 annotated steps and a  $720 \times 540$  resolution, divided into 50, 10, and 40 videos for

**Table 1.** Comparison of CSMAE with other state-of-the-art methods under different data-regime settings on the D99 dataset[5].

Methods	Pre-training Dataset	Masking	Data Regime (%)			
			10	25	50	100
MaskFeat [13]	Kinetics-400	Random	47.28	59.32	60.47	72.85
GLSFormer [14]	Kinetics-400	-	47.19	61.54	63.76	<b>80.24</b>
VideoMAE [9]	D-450	Frame	48.62	58.73	60.84	70.91
STMAE [15]	D-450	Random	52.37	60.42	63.58	74.16
VideoMAE [9]	Kinetics-400	Tube	46.16	59.76	60.99	73.35
VideoMAE [9]	D-450	Random	50.24	60.89	62.34	72.98
VideoMAE [9]	D-450	Tube	52.11	61.59	63.72	74.39
CSMAE	D-450	Token Selection	<b>54.75</b>	<b>63.12</b>	<b>65.83</b>	78.14

**Table 2.** Quantitative results of step recognition from different methods on the D99 and Cataract-101 datasets.

Method	D99				Cataract-101			
	Jaccard	Precision	Recall	Accuracy	Jaccard	Precision	Recall	Accuracy
ResNet[16]	37.98 $\pm$ 2.97	54.76 $\pm$ 2.77	52.28 $\pm$ 2.89	72.06 $\pm$ 2.12	62.58 $\pm$ 1.92	76.68 $\pm$ 1.86	74.73 $\pm$ 1.27	82.64 $\pm$ 1.54
SV-RCNet[17]	39.15 $\pm$ 2.03	58.18 $\pm$ 1.67	54.25 $\pm$ 1.86	73.39 $\pm$ 1.64	66.51 $\pm$ 1.30	84.96 $\pm$ 0.94	76.61 $\pm$ 1.18	86.13 $\pm$ 0.91
OHFM[18]	40.01 $\pm$ 1.68	59.12 $\pm$ 1.33	55.49 $\pm$ 1.63	73.82 $\pm$ 1.13	69.01 $\pm$ 0.93	85.37 $\pm$ 0.78	78.29 $\pm$ 0.81	87.82 $\pm$ 0.71
TeCNO[19]	41.31 $\pm$ 1.72	61.56 $\pm$ 1.41	55.81 $\pm$ 1.58	74.07 $\pm$ 1.78	70.18 $\pm$ 1.15	86.03 $\pm$ 0.83	79.52 $\pm$ 0.90	88.26 $\pm$ 0.92
TMRNet[20]	41.42 $\pm$ 1.76	61.37 $\pm$ 1.46	56.02 $\pm$ 1.65	75.11 $\pm$ 0.91	71.83 $\pm$ 0.91	85.09 $\pm$ 0.72	82.44 $\pm$ 0.75	89.68 $\pm$ 0.76
Trans-SVNet[21]	42.06 $\pm$ 1.51	60.12 $\pm$ 1.55	56.36 $\pm$ 1.24	74.89 $\pm$ 1.37	72.32 $\pm$ 1.04	86.72 $\pm$ 0.85	81.12 $\pm$ 0.93	89.45 $\pm$ 0.88
ViT[10]	38.18 $\pm$ 2.79	55.15 $\pm$ 2.42	53.60 $\pm$ 2.63	72.45 $\pm$ 1.91	64.77 $\pm$ 1.97	78.51 $\pm$ 1.42	75.62 $\pm$ 1.83	84.56 $\pm$ 1.72
TimesFormer[22]	42.69 $\pm$ 1.34	64.24 $\pm$ 1.20	55.17 $\pm$ 1.26	77.83 $\pm$ 0.96	75.97 $\pm$ 1.26	<b>85.38 <math>\pm</math> 0.93</b>	84.47 $\pm$ 0.95	90.76 $\pm$ 1.05
STMAE[15]	41.67 $\pm$ 1.29	59.38 $\pm$ 2.46	53.22 $\pm$ 1.78	74.16 $\pm$ 1.39	70.54 $\pm$ 1.63	81.47 $\pm$ 2.35	78.67 $\pm$ 1.54	85.29 $\pm$ 1.62
VideoMAE[9]	42.58 $\pm$ 1.73	61.24 $\pm$ 1.20	56.35 $\pm$ 1.82	74.39 $\pm$ 1.47	71.39 $\pm$ 1.25	82.13 $\pm$ 1.39	80.16 $\pm$ 1.68	86.47 $\pm$ 1.52
CSMAE	<b>43.51 <math>\pm</math> 1.47</b>	<b>64.32 <math>\pm</math> 1.36</b>	<b>52.45 <math>\pm</math> 1.17</b>	<b>78.14 <math>\pm</math> 1.25</b>	<b>76.82 <math>\pm</math> 2.27</b>	84.26 $\pm$ 1.64	<b>86.73 <math>\pm</math> 1.38</b>	89.83 $\pm$ 1.15

training, validation, and testing [5]. All videos are subsampled to 1 fps and resized to  $250 \times 250$  for pre-training and fine-tuning, as in prior studies [21, 26].

**Evaluation Metrics.** To compare the results of CSMAE on step recognition, following [5, 27] we estimated accuracy, precision, recall, and Jaccard index.

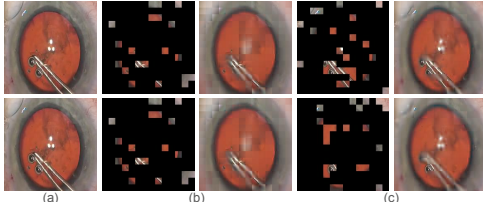


**Fig. 2.** Qualitative Comparison of Reconstructed Images after Pre-training Experiment. (a) indicates Original Images, (b) indicates Mask and Reconstructed Image from VideoMAE[9] and (c) indicates Selected Masks from TSN and Reconstructed Image from CSMAE.

**Comparison with state-of-the-art methods.** Table 1 compares our CSMAE model with state-of-the-art pre-training and fine-tuning methods across multiple data-regime settings on the D99 dataset. Although VideoMAE [9] was trained with 90% masking, our CSMAE achieves consistently strong performance with a 95% masking ratio. Against other pre-training methods like MaskFeat [13], STMAE [15], and variations of VideoMAE, we observe gains of up to 7% with fewer data.

In both high- and low-data regimes, our model performs comparably or better than specialized step recognition models like GLSFormer [5]. Notably, at 10% labeled data,

CSMAE shows an improvement of about 8%, reflecting the effectiveness of the Token Selection Network in focusing on high-informative spatiotemporal regions.

Furthermore, our model demonstrates strong transferability on the Cataract-101 dataset (Table 2), achieving up to 3–5% improvements in Jaccard and recall over pre-training methods like STMAE, VideoMAE, and specialized networks such as Trans-SVNet and TimesFormer, highlighting the generalizability of the learned features across different surgical settings.

**Qualitative Results.** Figure 2 compares VideoMAE [9] and our CSMAE approach, illustrating masked tokens and frame reconstruction quality in cataract videos. VideoMAE (b) uses a consistent tube masking across frames, whereas our CSMAE (c) applies a dynamic, frame-specific masking pattern, enhancing the capture of spatial and temporal details.

Despite VideoMAE’s lower masking ratio (90%), its reconstructed frames show noticeable blurriness, while our method, even with a 95% masking ratio, preserves finer details like cataract textures and surgical bubbles, indicating higher fidelity in critical feature representation.

Additionally, CSMAE’s mask distribution aligns with non-uniform sampling, prioritizing tokens from high-information regions, such as surgical instruments and cataract morphology, over the static background, demonstrating its ability to focus on regions with significant spatiotemporal changes.

**Ablation Studies.** We ablate the CSMAE design by evaluating its performance on the VVT architecture for semi-supervised step recognition with 10% labeled data. Our analysis focuses on masking strategies, decoder depths, masking ratios, and loss functions.

*Masking Strategies:* Table 3c shows that random patch

**Table 3.** Ablation studies on step-recognitions in semi-supervised setting (10% labeled data) using Video-Vision Transformer as a backbone. (a) Different Masking Ratio: CSMAE works well with extremely high masking ratio, models are trained for 800 epochs. (b) Decoder Depth: CSMAE performs the best with 4 blocks of decoder, models are trained for 800 epochs with a masking ratio of 95%. (c) Mask sampling: CSMAE outperforms random, frame, and tube masking. (d) Pre-training epochs: Better performance is achieved during fine-tuning when pre-trained for more epochs. (e) Loss function: CSMAE performs best with MSE loss (normalized) and  $L_S$ , models are trained for 800 epochs with a masking ratio of 95%.

Ratio	mAP	Blocks	mAP	Case	mAP	Epochs	mAP	Case	mAP
0.98	52.47	1	50.69	Random	50.53	200	50.28	L1 (w / norm)	53.62
0.95	<b>54.75</b>	2	52.34	Tube	52.19	400	52.42	L1 (wout / norm)	52.56
0.90	53.85	4	<b>54.75</b>	Frame	43.92	600	53.97	MSE (w / norm)	<b>54.75</b>
0.80	50.82	8	53.68	CSMAE	<b>54.75</b>	800	<b>54.75</b>	MSE (wout / norm)	52.89

masking (50.52%) and tube masking [9] (51.19%) outperform frame-based masking (43.92%). Adaptive token sampling, maximizing reconstruction error, achieves the highest mAP (54.75%) with a 95% masking ratio, surpassing random masking at 90%.

*Decoder Depth:* As shown in Table 3b, increasing decoder blocks from 1 to 4 improves mAP from 50.69% to 54.75%, with performance declining beyond four blocks, suggesting an optimal depth of 4 for balancing complexity and efficiency, consistent with VideoMAE [9].

*Loss Function and Training Epochs:* Table 3e indicates L1/MSE loss on normalized pixels outperforms raw pixel loss. Table 3d shows a 4.5% accuracy improvement by extending pretraining epochs from 200 to 800, highlighting the benefits of longer training.

## 4. CONCLUSION

In this paper, we present a novel masking technique, CSMAE, tailored for Masked Autoencoder (MAE)-based pretraining on cataract surgical videos to enhance spatiotemporal representation learning. Our approach, designed for Video Vision Transformer models, uses a pretraining dataset of over 350 untrimmed surgical videos (avg. 34 minutes each) to prepare models for fine-tuning on downstream tasks with minimal labels. Qualitative analysis shows that our sampling method surpasses competing masking strategies in both supervised and semi-supervised settings on cataract surgery tasks, highlighting its potential for broader clinical applications.

## 5. ACKNOWLEDGMENTS

This research was supported by a grant from the National Institutes of Health, USA; R01EY033065. The content is solely the responsibility of the authors and does not necessarily represent the official views of the National Institutes of Health.

## 6. REFERENCES

- [1] Qingbo Kang, Jun Gao, Kang Li, and Qicheng Lao, “Deblurring masked autoencoder is better recipe for ultrasound image recognition,” *arXiv preprint arXiv:2306.08249*, 2023.
- [2] Mengkang Lu, Tianyi Wang, and Yong Xia, “Multi-modal pathological pre-training via masked autoencoders for breast cancer diagnosis,” in *International Conference on Medical Image Computing and Computer-Assisted Intervention*. Springer, 2023, pp. 457–466.
- [3] Benedikt Boecking, Naoto Usuyama, et al., “Making the most of text semantics to improve biomedical vision-language processing,” in *ECCV*. Springer, 2022, pp. 1–21.
- [4] Jong Hak Moon, Hyungyung Lee, Woncheol Shin, Young-Hak Kim, and Edward Choi, “Multi-modal understanding and generation for medical images and text via vision-language pre-training,” *IEEE Journal of Biomedical and Health Informatics*, vol. 26, no. 12, pp. 6070–6080, 2022.
- [5] Nisarg A Shah, Shameema Sikder, S Swaroop Vedula, and Vishal M Patel, “Glsformer: Gated-long, short sequence transformer for step recognition in surgical videos,” in *MICCAI*. Springer, 2023, pp. 386–396.
- [6] Kai Hu, Jie Shao, Yuan Liu, Bhiksha Raj, Marios Savvides, and Zhiqiang Shen, “Contrast and order representations for video self-supervised learning,” in *Proceedings of the IEEE/CVF International Conference on Computer Vision*, 2021, pp. 7939–7949.
- [7] Jungin Park, Jiyoung Lee, Ig-Jae Kim, and Kwanghoon Sohn, “Probabilistic representations for video contrastive learning,” in *Proceedings of the IEEE/CVF Conference on Computer Vision and Pattern Recognition*, 2022, pp. 14711–14721.
- [8] Kaiming He, Xinlei Chen, Saining Xie, Yanghao Li, Piotr Dollár, and Ross Girshick, “Masked autoencoders

are scalable vision learners,” in *Proceedings of the IEEE/CVF conference on computer vision and pattern recognition*, 2022, pp. 16000–16009.

[9] Zhan Tong, Yibing Song, Jue Wang, and Limin Wang, “Videomae: Masked autoencoders are data-efficient learners for self-supervised video pre-training,” *Advances in neural information processing systems*, vol. 35, pp. 10078–10093, 2022.

[10] Alexey Dosovitskiy, Lucas Beyer, Alexander Kolesnikov, Dirk Weissenborn, Xiaohua Zhai, Thomas Unterthiner, Mostafa Dehghani, Matthias Minderer, Georg Heigold, Sylvain Gelly, et al., “An image is worth 16x16 words: Transformers for image recognition at scale,” *arXiv preprint arXiv:2010.11929*, 2020.

[11] Anurag Arnab, Mostafa Dehghani, Georg Heigold, Chen Sun, Mario Lučić, and Cordelia Schmid, “Vivit: A video vision transformer,” in *Proceedings of the IEEE/CVF international conference on computer vision*, 2021, pp. 6836–6846.

[12] Wele Gedara Chaminda Bandara, Naman Patel, Ali Gholami, Mehdi Nikkhah, Motilal Agrawal, and Vishal M Patel, “Adamae: Adaptive masking for efficient spatiotemporal learning with masked autoencoders,” in *Proceedings of the IEEE/CVF Conference on Computer Vision and Pattern Recognition*, 2023, pp. 14507–14517.

[13] Chen Wei, Haoqi Fan, Saining Xie, Chao-Yuan Wu, Alan Yuille, and Christoph Feichtenhofer, “Masked feature prediction for self-supervised visual pre-training,” in *Proceedings of the IEEE/CVF Conference on Computer Vision and Pattern Recognition*, 2022, pp. 14668–14678.

[14] Nisarg A Shah and Gaurav Bharaj, “Towards device efficient conditional image generation,” *arXiv preprint arXiv:2203.10363*, 2022.

[15] Christoph Feichtenhofer, Yanghao Li, Kaiming He, et al., “Masked autoencoders as spatiotemporal learners,” *Advances in neural information processing systems*, vol. 35, pp. 35946–35958, 2022.

[16] Kaiming He, Xiangyu Zhang, Shaoqing Ren, and Jian Sun, “Deep residual learning for image recognition,” in *Proceedings of the IEEE conference on computer vision and pattern recognition*, 2016, pp. 770–778.

[17] Yueming Jin, Qi Dou, Hao Chen, Lequan Yu, Jing Qin, Chi-Wing Fu, and Pheng-Ann Heng, “Sv-rcnet: workflow recognition from surgical videos using recurrent convolutional network,” *IEEE transactions on medical imaging*, vol. 37, no. 5, pp. 1114–1126, 2017.

[18] Fangqiu Yi and Tingting Jiang, “Hard frame detection and online mapping for surgical phase recognition,” in *MICCAI 2019*. Springer, 2019, pp. 449–457.

[19] Tobias Czempiel, Magdalini Paschali, Matthias Keicher, Walter Simson, Hubertus Feussner, Seong Tae Kim, and Nassir Navab, “Tecno: Surgical phase recognition with multi-stage temporal convolutional networks,” in *MICCAI 2020*. Springer, 2020, pp. 343–352.

[20] Yueming Jin, Yonghao Long, Cheng Chen, Zixu Zhao, Qi Dou, and Pheng-Ann Heng, “Temporal memory relation network for workflow recognition from surgical video,” *IEEE Transactions on Medical Imaging*, vol. 40, no. 7, pp. 1911–1923, 2021.

[21] Xiaojie Gao, Yueming Jin, Yonghao Long, Qi Dou, and Pheng-Ann Heng, “Trans-svnet: Accurate phase recognition from surgical videos via hybrid embedding aggregation transformer,” in *MICCAI 2021*. Springer, 2021, pp. 593–603.

[22] Gedas Bertasius, Heng Wang, and Lorenzo Torresani, “Is space-time attention all you need for video understanding?,” in *ICML*, 2021, vol. 2, p. 4.

[23] Ronald J Williams, “Simple statistical gradient-following algorithms for connectionist reinforcement learning,” *Machine learning*, vol. 8, pp. 229–256, 1992.

[24] Klaus Schoeffmann, Mario Taschwer, Stephanie Sarny, Bernd Münzer, Manfred Jürgen Primus, and Doris Putzgruber, “Cataract-101: video dataset of 101 cataract surgeries,” in *Proceedings of the 9th ACM multimedia systems conference*, 2018, pp. 421–425.

[25] Felix Yu, Gianluca Silva Croso, Tae Soo Kim, Ziang Song, Felix Parker, Gregory D Hager, Austin Reiter, S Swaroop Vedula, Haider Ali, and Shameema Sikder, “Assessment of automated identification of phases in videos of cataract surgery using machine learning and deep learning techniques,” *JAMA network open*, vol. 2, no. 4, pp. e191860–e191860, 2019.

[26] Andru P Twinanda, Sherif Shehata, Didier Mutter, Jacques Marescaux, Michel De Mathelin, and Nicolas Padoy, “Endonet: a deep architecture for recognition tasks on laparoscopic videos,” *IEEE transactions on medical imaging*, vol. 36, no. 1, pp. 86–97, 2016.

[27] Tae Soo Kim, Molly O’Brien, Sidra Zafar, Gregory D Hager, Shameema Sikder, and S Swaroop Vedula, “Objective assessment of intraoperative technical skill in capsulorhexis using videos of cataract surgery,” *International journal of computer assisted radiology and surgery*, vol. 14, no. 6, pp. 1097–1105, 2019.